Molecular Biology of the Cell
Vol. 12, 2894–2905, September 2001

Mammalian Dynamin-like Protein DLP1 Tubulates Membranes

Yisang Yoon, Kelly R. Pitts, and Mark A. McNiven*

Center for Basic Research in Digestive Diseases and Department of Biochemistry and Molecular Biology, Mayo Clinic, Rochester, Minnesota 55905

Submitted November 13, 2000; Revised April 3, 2001; Accepted June 26, 2001
Monitoring Editor: Juan Bonifacino

Dynamins are large GTPases with mechanochemical properties that are known to constrict and tubulate membranes. A recently identified mammalian dynamin-like protein (DLP1) is essential for the proper cellular distribution of mitochondria and the endoplasmic reticulum in cultured cells. In this study, we investigated the ability of DLP1 to remodel membranes similar to conventional dynamin. We found that the expression of a GTPase-defective mutant, DLP1-K38A, in cultured cells led to the formation of large cytoplasmic aggregates. Electron microscopy (EM) of cells expressing DLP1-K38A revealed that these aggregates were comprised of membrane tubules of a consistent diameter. High-magnification EM revealed the presence of many regular striations along individual membrane tubules, and immunogold labeling confirmed the association of DLP1 with these structures. Biochemical experiments with the use of recombinant DLP1 and labeled GTP demonstrated that DLP1-K38A binds but does not hydrolyze or release GTP. Furthermore, the affinity of DLP1-K38A for membrane is increased compared with wild-type DLP1. To test whether DLP1 could tubulate membrane in vitro, recombinant DLP1 was combined with synthetic liposomes and nucleotides. We found that DLP1 protein alone assembled into sedimentable macromolecular structures in the presence of guanosine-5′-*O*-(3-thio)triphosphate (GTPγS) but not GTP. EM of the GTPγS-treated DLP1 revealed clusters of stacked helical ring structures. When liposomes were included with DLP1, formation of long membrane tubules similar in size to those formed in vivo was observed. Addition of GTPγS greatly enhanced membrane tubule formation, suggesting the GTP-bound form of DLP1 deforms liposomes into tubules as the DLP1-K38A does in vivo. These results provide the first evidence that the dynamin family member, DLP1, is able to tubulate membranes both in living cells and in vitro. Furthermore, these findings also indicate that despite the limited homology to conventional dynamins (35%) these proteins remodel membranes in a similar manner.

INTRODUCTION

The large GTPase dynamin has been implicated in intracellular membrane trafficking by its ability to tubulate and vesiculate membrane at the plasma membrane (Herskovits *et al.*, 1993; van der Bliek *et al.*, 1993; Damke *et al.*, 1994), *trans*-Golgi network (Henley and McNiven, 1996; Maier *et al.*, 1996; Jones *et al.*, 1998), and endosomes (Llorente *et al.*, 1998; Nicoziani *et al.*, 2000). Although the precise function of dynamin in these membrane-trafficking processes is still controversial, recent in vitro studies have indicated that dynamin has the capacity to tubulate spherical liposomes and, upon GTP hydrolysis, constrict, deform, or sever membrane tubules into discrete vesicles (Sweitzer and Hinshaw, 1998; Takei *et al.*, 1998; Stowell *et al.*, 1999; Takei *et al.*, 1999). These biochemical observations suggest that dynamin is a mechanochemical enzyme that acts in the final stages of vesicle formation (McNiven, 1998; McNiven *et al.*, 2000). DLP1, an 80-kDa dynamin-like protein recently identified by several groups, has an N-terminal GTPase domain highly homologous to that of the conventional dynamins (Shin *et al.*, 1997; Imoto *et al.*, 1998; Kamimoto *et al.*, 1998; Smirnova *et al.*, 1998; Yoon *et al.*, 1998), suggesting that DLP1 has a similar enzymatic activity. Although this protein does not have a pleckstrin homology or proline-rich domain as dynamin does, the C-terminal coiled-coil region of DLP1 has significant homology to the dynamin GED domain (Sever *et al.*, 1999), indicating a similar GTPase regulation and multimeric configuration to that of dynamin. Recent studies with the use of yeast two-hybrid assays and biochemical analyses suggest that DLP1 forms a homotetrameric complex similar to dynamin (Shin *et al.*, 1999). These similarities predict that DLP1 may function via a mechanochemical activity similar to dynamin. DLP1 has been localized to mitochondria and

* Corresponding author. E-mail address: mcniven.mark@mayo.edu.

other cellular organelles (Yoon *et al.*, 1998; Pitts *et al.*, 1999) and is suggested to function in the maintenance of mitochondrial morphology (Smirnova *et al.*, 1998; Labrousse *et al.*, 1999; Pitts *et al.*, 1999).

In a previous study, we reported that DLP1 mutants exhibit an altered cytoplasmic distribution (Pitts *et al.*, 1999). DLP1 harboring a lysine-to-alanine (K38A) mutation in GTP-binding element 1 assembled into large cytoplasmic aggregates in addition to associating with punctate vesicular structures similar to wild-type DLP1. In contrast, DLP1 containing an aspartate-to-asparagine (D231N) mutation in GTP-binding element 3 did not localize to any cellular structure and appeared diffusely cytosolic, suggesting a loss of membrane targeting. Taken together, these data suggested that DLP1 associates with membranes in a GTP-dependent manner.

In this study, we have tested whether DLP1 has the capacity to bind and tubulate membranes in living cells and in vitro. Examination of the cytoplasmic aggregates that accumulate in cells expressing DLP1-K38A by thin section electron microscopy (EM) revealed that these aggregates are comprised of tubular membrane clusters that are coated with DLP1 in a periodic manner. Consistent with these in vivo observations, we also found that recombinant DLP1-K38A protein is capable of binding GTP but is deficient in hydrolysis, stimulating DLP1 to bind and tubulate membranes. Additional in vitro studies demonstrated that DLP1 assembled into stacks of ring structures and, upon addition of liposomes, induced the formation of lipid tubules in a nucleotide-dependent manner, similar to the DLP1-K38A mutant protein in living cells. To our knowledge, these findings provide the first demonstration that a dynamin family member, DLP1, is able to tubulate membranes both in living cells and in vitro.

MATERIALS AND METHODS

Cell Culture, DNAs, Transfection

Cell lines Clone 9 (ATCC CRL-1439) and BHK-21 (ATCC CCL-10) were used for all experiments. Cells were maintained at 37°C, 5% CO_2 in Ham's F-12K medium for Clone 9 and in DMEM for BHK-21 cells, supplemented with 10% fetal bovine serum, 100 U/ml penicillin, and 100 μg/ml streptomycin (Life Technologies, Bethesda, MD). The point mutants DLP1-K38A and DLP1-D231N were described previously (Pitts *et al.*, 1999). BHK-21 cells stably expressing YFP-Sec61β and DNA construct for green fluorescent protein (GFP)-ADP/ATP translocase were generous gifts from Dr. Tom Rapoport (Harvard University, Cambridge, MA) and the GFP-TGN38 plasmid was constructed in our laboratory. Glutathione *S*-transferase (GST)-tagged wild type (WT), K38A, and D231N were generated by cloning DLP1-WT, K38A, or D231N into pGEX-3X (Amersham Pharmacia Biotech, Piscataway, NJ) with the use of *Bam*HI (5′ end; New England Biolabs, Beverly, MA) and *Eco*RI (3′ end; Life Technologies) in-frame with GST at the N-terminal end of the constructs. For cell transfection, DNA constructs were purified with the use of plasmid purification columns (QIAGEN, Hilden, Germany). Cells were plated 16–24 h before transfection on glass coverslips in 35-mm tissue culture dishes. Transfections were performed either by with the use of LipofectAMINE (Life Technologies) per the manufacturer's instructions or by microinjecting DNA into the nucleus as described (Pitts *et al.*, 1999). Transfected cells were allowed to recover for 16–24 h before processing for either immunofluorescence or EM.

Immunofluorescence

Indirect immunofluorescence was performed as described elsewhere (Henley and McNiven, 1996; Yoon *et al.*, 1998). Briefly, cells were fixed and permeabilized and then incubated in a blocking buffer containing 5% goat serum for 1 h at 37°C. The rabbit polyclonal antibody DLP-N (Yoon *et al.*, 1998) and Texas Red-conjugated goat anti-rabbit IgG (Molecular Probes, Eugene, OR) were used for primary and secondary antibodies, respectively. After appropriate rinsings, coverslips were mounted in ProLong antifade reagent (Molecular Probes) on glass slides and cells were viewed with a Zeiss Axiovert 35 epifluorescence microscope (Carl Zeiss, Thornwood, NJ) equipped with a 100× objective (Zeiss Plan-Neofluar; numerical aperture 1.30). Phase and fluorescence images were acquired with a Sensys cooled charge-coupled device (Photometrics, Tucson, AZ) driven by Metamorph 3.6 imaging software (Universal Imaging, West Chester, PA).

EM

Cells were plated on etched grid coverslips with numbered imprints (BELLCO Biotechnology, Vineland, NJ). Cells within four adjacent squares on the coverslip were microinjected with DLP1-WT or mutant DNA constructs. After 24 h, cells were rinsed with 37°C phosphate-buffered saline (PBS), submerged sequentially in primary fixative (100 mM Na-PO_4, pH 7.2, 50 mM sucrose, 3.0% glutaraldehyde) for an hour, in 1% osmium tetroxide for 30 min, and in 1% uranyl acetate for 30 min. Fixed cells were then dehydrated in a graded series of ethanol, and embedded in Quetol 651 (Ted Pella, Redding, CA). The block face of the resin was then trimmed to leave square boxes that contain only injected cells and processed as described previously (Henley *et al.*, 1998). For immunogold labeling, cells expressing GFP-DLP1-K38A were processed in one of two ways. To preserve DLP1 antigenicity, cells were fixed in 4% formaldehyde (Ted Pella) and 0.2% gluteraldehyde (EM Science, Gibbstown, NJ) in Dulbecco's PBS (D-PBS; Sigma, St. Louis, MO). After fixation, cells were dehydrated in a graded series of ethanol on ice (60%, 15 min; 70%, 30 min) and then at −20°C (80%, 30 min; 95%, 15 min; 100%, 15 min). After dehydration, ethanol was exchanged with LR White (Ted Pella; 60 min at −20°C, overnight at −20°C) and samples were then embedded for 3 d at 55°C. To preserve ultrastructure, cells were processed and embedded in Quetol 651 as described above and subjected to antigen retrieval by deplasticizing (Stirling and Graff, 1995). Briefly, samples were dipped in a saturated sodium ethoxide solution (40 s) and then rinsed in a graded series of ethanol to water. Samples were then treated with saturated sodium metaperiodiate for 40 min and rinsed extensively in water. Immunogold labeling was performed on thin sections with the use of the DLP-N polyclonal antibody diluted in blocking buffer (D-PBS, 0.05% Tween 20, 2% goat serum, 0.15 M glycine). After four rinses, the DLP-N primary antibody was detected with the use of 15-nm gold-conjugated goat anti-rabbit secondary antibody (Amersham Pharmacia Biotech). For negative staining of in vitro tubulation, a drop of sample was adsorbed onto a Formvar-coated copper grid. After removing excess liquid, grids were rinsed with buffer A (20 mM HEPES, pH 7.2, 100 mM KCl, 2 mM $MgCl_2$, 1 mM dithiothreitol) and stained with three consecutive drops of 1.0% uranyl acetate solution. Samples were viewed and photographed with the use of a JEOL 1200 electron microscope.

GTP Binding and Hydrolysis

GST-fusion proteins were isolated from bacteria expressing full-length GST-tagged WT, K38A, or D231N. Bacteria harboring fusion constructs were induced by 100 μM isopropyl β-D-thiogalactoside for 16–18 h at room temperature to overproduce recombinant proteins. Soluble bacterial extracts were obtained by an intensive sonication in buffer A containing 1.0% TX-100 and protease inhibitors (Complete; Roche Molecualr Biochemicals, Indianapolis, IN) followed by centrifugation at 15,000 × g for 20 min. Bacterial extracts

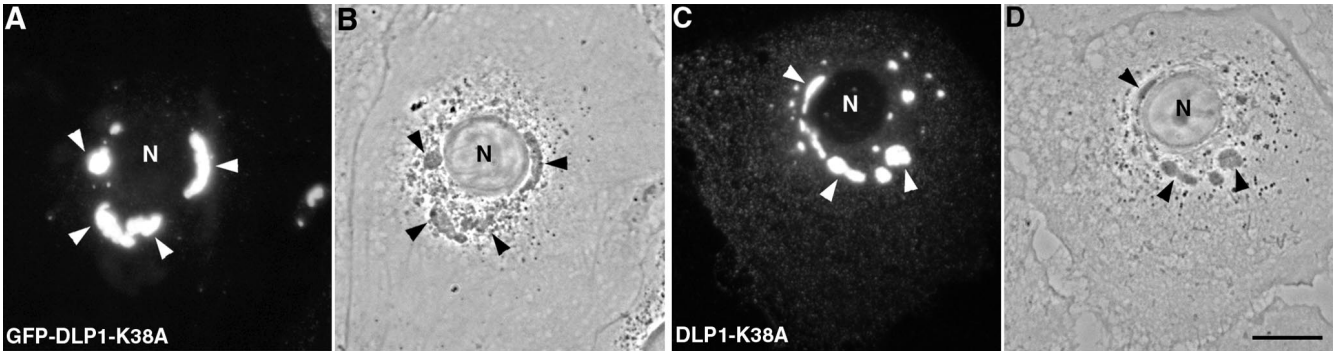

Figure 1. Expression of a specific DLP1 mutant (DLP1-K38A) in cultured cells induces the formation of large DLP1-containing structures. Clone 9 cells were transfected to express either GFP-tagged DLP1-K38A (A) or untagged DLP1-K38A (C). Untagged DLP1 was detected by immunofluorescence microscopy with anti-DLP1 antibodies (C). Both untagged and GFP-tagged mutant DLP1 formed large fluorescent DLP1-containing structures (arrowheads). These were readily visible as dense structures in the cytoplasm by phase contrast microscopy (B and D, arrowheads). Bar, 10 μm.

were incubated with glutathione-conjugated sepharose beads (Sigma) for 3 h at 4°C with gentle rotation to isolate recombinant proteins. Beads carrying GST-fusion proteins were obtained by washing five times with excess buffer A with 0.1% TX-100. To test for GTP binding to DLP1, 25 nM of either [γ-^{35}S]guanosine-5′-*O*-(3-thio)triphosphate (GTPγS) or [α-^{32}P]GTP was incubated with 5 μM fusion protein bound to beads in buffer A at room temperature. After periods of incubation, beads were washed and collected by brief centrifugation and radioactivity was counted in a liquid scintillation counter. The data were expressed as percentage of binding relative to the value obtained with DLP1-WT at 10 min. For the test of GTP hydrolysis by DLP1, fusion proteins were eluted from beads by 50 mM glutathione and eluates were dialyzed against buffer A overnight. The reaction mixture for hydrolysis contained 5 μM DLP1 protein, 0.05% bovine serum albumin, and 84 nM [α-^{32}P]GTP in buffer A. At each time point, 1.0 μl of reaction was taken and spotted on PEI-cellulose (Fisher Scientific, Pittsburgh, PA) and nucleotides were separated by thin-layer chromatography (TLC) with 1.0 M LiCl. Radioactive spots were quantitated by with the use of a phosphorimager and ImageQuant software (Molecular Dynamics, Sunnyvale, CA). GTP hydrolysis was expressed as ratio of GDP to total nucleotide (GDP + GTP) at each time point.

Membrane-Protein Cosedimentation Assay

Rat liver total membranes were obtained by pelleting the postnuclear supernatant from a liver homogenate. Peripherally attached proteins were removed by resuspending and washing total membranes twice in 100 mM Na_2CO_3, pH 11.75. The resulting stripped membranes were stored in buffer A containing 0.25 M sucrose. GST-DLP1 proteins prepared as described above were precleared before incubation with membranes by centrifugation at 39,000 $\times$ *g* at 4°C. Proteins and membranes were mixed to final concentrations of 60 and 250 μg/ml, respectively, and incubated at 37°C for 30 min in the presence of 1.0 mM GTP in buffer A containing 0.25 M sucrose. Membrane–protein complexes were then pelleted at 39,000 $\times$ *g* at room temperature for 30 min, separated by SDS-PAGE, and analyzed by immunoblotting with an anti-DLP1 antibody.

Purification of DLP1 and In Vitro Liposome Tubulation

DLP1 cDNA was cloned into the pRSET vector (Invitrogen, Carlsbad, CA) to overexpress 6-His-tagged DLP1. The 6-His-tagged DLP1 was purified with ProBond-resin (Invitrogen) according to the manufacturer's instructions. Briefly, bacteria carrying a plasmid for 6-His-tagged DLP1 were induced with 0.5 mM isopropyl β-D-thiogalactoside for 16–18 h at room temperature to overproduce DLP1. Soluble bacterial extracts were obtained by sonication followed by centrifugation at 15,000 $\times$ *g* for 20 min. Bacterial extracts were incubated with Ni^+-resin (ProBond; Invitrogen) for 30 min at 4°C with gentle rotation to isolate DLP1 proteins. After rinsing the resin, 6-His-DLP1 was eluted with 500 mM imidazole. Eluted protein was equilibrated with buffer A before reactions for self-assembly and liposome tubulation. For DLP1 polymerization, 6-His-DLP1 was incubated with or without nucleotide at 37°C for 30 min and the reaction mixture was centrifuged at 100,000 $\times$ *g* for 30 min at room temperature. Liposomes were prepared from either Folch fraction III (Sigma) or synthetic phosphatidylserine (PS) (1,2-dioleoyl-sn-glycero-3-[phospho-L-serine]; Avanti Polar Lipids, Birmingham, AL). Lipids were dried under nitrogen and resuspended in buffer A then extruded 10 times through polycarbonate filters with 1.0-μm pores (Nucleopores). For liposome tubulation, DLP1 (0.5–1.0 mg/ml) was mixed with liposomes (0.5 mg/ml) and nucleotide (0.5 mM), and the mixture was incubated at 37°C for 30 min. The resulting reaction mixture was then processed for EM as described.

RESULTS

Expression of DLP1-K38A in Cultured Mammalian Cells Induces Formation of DLP1-containing Aggregates

In a previous study (Pitts *et al.*, 1999), we expressed a mutant DLP1 (DLP1-K38A) in cultured mammalian cells in an attempt to define the function of this dynamin family member. We observed that the expression of this mutant tagged with GFP induced the formation of large fluorescent cytoplasmic structures. As shown in Figure 1A, Clone 9 cells, a normal rat liver cell line, transiently transfected with GFP-DLP1-K38A contained large green fluorescent DLP1 aggregates that varied in size and shape. It was possible that the GFP tag on the protein might have caused a structural malformation and formed aberrant protein aggregates. However, these structures were not found in cells expressing wild-type DLP1 or a different DLP1 point mutant also tagged with GFP (Pitts *et al.*, 1999), suggesting that the formation of this structure is attributed to the K38A mutation in DLP1. To confirm that the DLP1-containing aggregates were not in-

duced by the GFP tag, an untagged DLP1-K38A construct was transfected and the cellular DLP1 detected by immunofluorescence with anti-DLP1 antibodies. As with GFP-DLP1-K38A, cells transfected with the untagged DLP1-K38A also contained large DLP1-positive structures (Figure 1C). The DLP1-K38A aggregates were readily detectable as dense structures by phase contrast microscopy shown in Figure 1, B and D.

Aggregates of DLP1-K38A Consist of Membrane Tubules Decorated with DLP1 Rings

To define the composition of fluorescent DLP1 structures in DLP1-K38A mutant cells, thin-section EM of cultured transfected cells was performed. Surprisingly, large tubular membrane clusters (TMCs) were frequently found in these transfected cells as shown in Figure 2. The TMCs were often situated in close apposition to residual ER cisternae and mitochondria (Figure 2, A and B) and were present only in cells expressing DLP1-K38A. Although these membrane clusters varied in size and shape, individual tubules within the clusters possessed remarkably consistent diameters (27 ± 3 nm), suggesting the presence of a rigid structural scaffolding along their length (Figure 2C). Further examination of the TMCs by higher magnification revealed the presence of periodic striations along the length of individual tubules (Figure 2D) reminiscent of the "collars" observed previously with the use of conventional dynamin in vitro (Takei *et al.*, 1995; Sweitzer and Hinshaw, 1998; Takei *et al.*, 1998, 1999; Stowell *et al.*, 1999). These EM observations suggested that DLP1 tubulates membranes by assembling into periodic rings viewed as striations along the length of the tubule. In higher magnification transmission electron microscopy (TEM) images, lipid bilayers were visible in many sections, indicating that the tubules were comprised of membrane (Figure 2E). As indicated with arrows in Figure 2E, a connection between the TMC and putative endoplasmic reticulum (ER) tubules was also evident. To further verify the presence of membrane in the TMC, and organelles or membrane populations that contribute to the formation of DLP1-tubular clusters, we induced the formation of TMCs in cells expressing GFP- or yellow fluorescent protein (YFP)-tagged resident membrane proteins of specific organelles. These included YFP-Sec61β for the ER membrane, GFP-ADP/ATP translocase for the mitochondrial membrane, and GFP-TGN38 for the *trans*-Golgi membrane. Although little or no GFP-ADP/ATP translocase and GFP-TGN38 were detected in TMCs, we found that the large TMCs contained significant amounts of YFP-Sec61β as shown in Figure 2, F and G. These results are consistent with the EM observations showing TMC-ER connections (Figure 2E). Furthermore, they support our previous observations (Pitts *et al.*, 1999) that mutants in DLP1 alter both mitochondrial and ER morphologies, while indicating that the ER membrane is a major source of the membrane of TMCs.

To verify that TMCs were comprised of DLP1 protein, we conducted immunoelectron microscopy of cells expressing the DLP1-K38A mutant with anti-DLP1 antibodies. Two different immunogold-labeling methods were used. A more mild fixation method provided better antigenic preservation and enabled detection of DLP1 on the TMCs (Figure 3A). Because fine structure was compromised in these preparations, we also more rigorously fixed the cells and then deplasticized the subsequent thin sections before incubation with antibodies (Figure 3B). In both methods, we found that TMCs were heavily labeled with gold particles. These immunogold-labeling results confirmed that the TMCs are indeed the large DLP1-positive structures seen by fluorescence microscopy.

DLP1-K38A Is Defective in GTP Hydrolysis with an Increased Affinity for Membranes

The observation that a single point mutation in the GTP-binding region of DLP1 induces the formation of TMCs suggests that GTP binding and hydrolysis of DLP1 may regulate the membrane binding of this protein. To characterize the K38A mutation, we tested the efficiency of GTP binding and hydrolysis of wild-type DLP1 (WT) and the two mutant proteins, DLP1-K38A and DLP1-D231N, which have been shown to induce formation of large cytoplasmic aggregates and a loss of membrane localization, respectively, when expressed in cultured cells (Pitts *et al.*, 1999). To test how these mutations might alter GTP hydrolysis, recombinant DLP1 proteins were incubated with radiolabeled GTP and reaction products were separated by TLC (Figure 4A). Efficiency of GTP hydrolysis was represented by percentage of GDP produced as shown in Figure 4B. Although WT hydrolyzed >70% of GTP to GDP within 60 min, both the K38A and D231N mutant proteins exhibited a complete loss of GTPase activity compared with WT. To determine whether this loss of GTPase activity in the mutant proteins was due to a lack of nucleotide binding, GTP binding of WT and mutant proteins was tested. When radiolabeled GTP was incubated with WT, K38A, or D231N proteins for increasing periods of time, the WT showed higher GTP binding at the early time point (10 min) and, as incubation time increased, WT-bound nucleotide decreased dramatically over the next 60 min (Figure 4C). This indicates that WT hydrolyzes and releases nucleotides over time, as expected. In contrast, DLP1-K38A initially showed low binding to GTP, which gradually increased over time (Figure 4C). DLP1-K38A showed an 8–10-fold increase in nucleotide binding over WT after prolonged incubation (120 min). These results suggest that DLP1-K38A is still capable of binding GTP but to a reduced extent (Figure 4C). Furthermore, DLP1-K38A is unable to release nucleotide owing to a defect in GTP hydrolysis (Figure 4B), resulting in accumulation of bound nucleotide in later time points. DLP1-D231N consistently showed an inability to bind GTP (Figure 4C), suggesting that the lack of GTPase activity of this mutant protein is probably due to loss of GTP binding. These results suggest that DLP1-K38A behaves as a GTP-bound protein when nucleotide is available, whereas DLP1-D231N is an "empty" mutant. It is well known that small GTPases that regulate membrane trafficking, such as Rabs, exhibit an increased affinity for membranes in the GTP-bound state (Donaldson and Klausner, 1994; Pfeffer, 1994). Accordingly, DLP1-K38A may associate with membranes more tightly than the WT protein. To test this prediction, we incubated either WT or DLP1-K38A with carbonate-stripped total liver membranes in the presence of GTP and examined membrane-binding ability by a cosedimentation assay. As shown in Figure 5, both WT and DLP1-K38A remained predominantly in the supernatant in the absence of membranes. However, upon incubation with membranes, the amount of

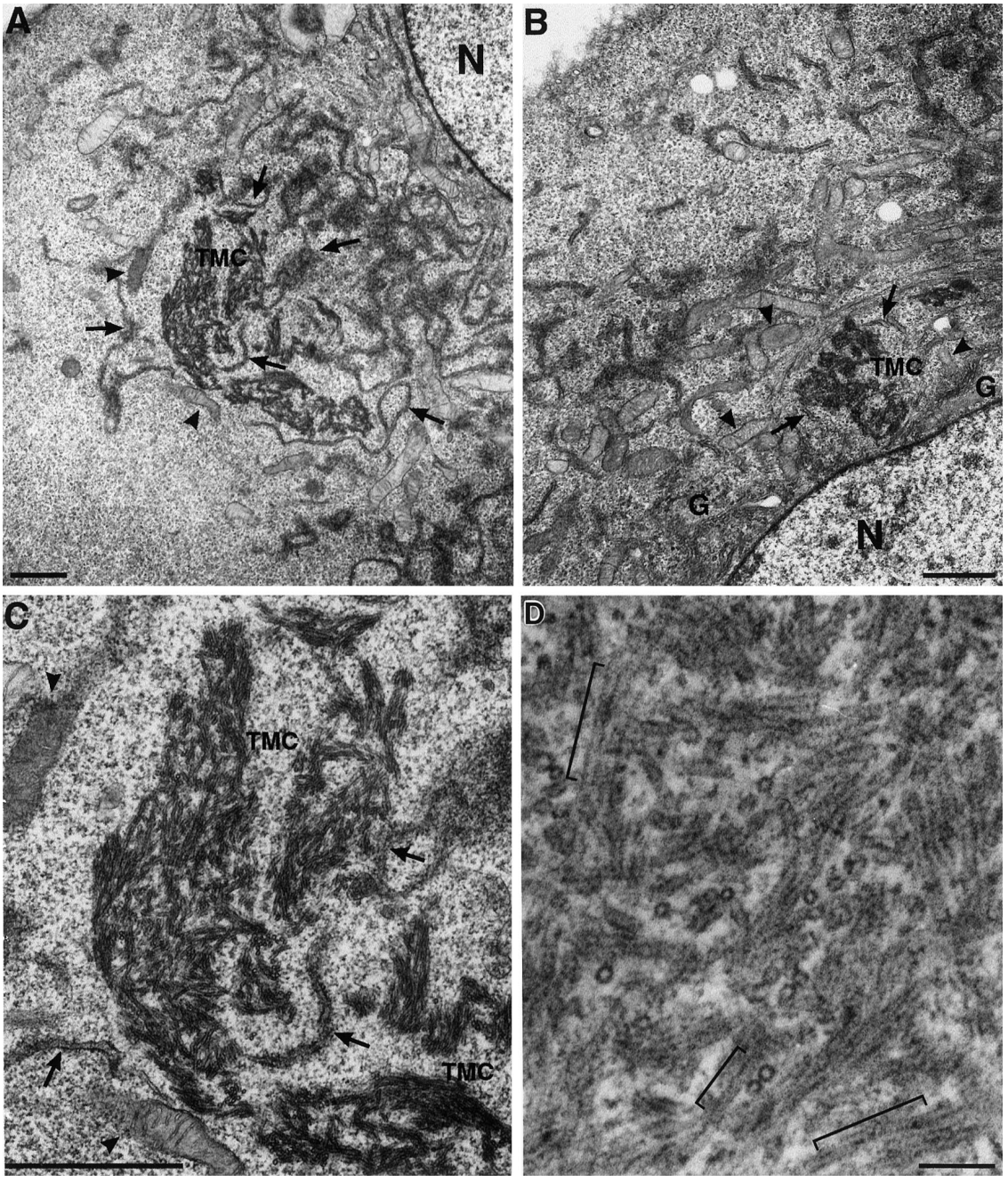

Figure 2. DLP1-K38A aggregates are comprised of constricted ER membrane tubules with periodic DLP1 striations. A plasmid encoding GFP-DLP1-K38A was microinjected into nuclei of BHK-21 (A–C) or Clone 9 (D) cells. 24 h after injection, cells were fixed, embedded, and subjected to thin-section electron microscopy. The peripheral cytoplasm of these cells display little ER or mitochondria. Instead, multiple TMCs are found in proximity to an atrophied endoplasmic reticulum (A–C, arrows) or collapsed mitochondria (A–C, arrowheads) near the nucleus. Higher magnification of a TMC from A reveals a complex network of membrane tubules (C) that exhibit a consistent uniform diameter. TMCs exhibit dense periodic striations or collars along the length of tubules (D). Higher magnification TEM image shows lipid bilayers in tubules (E). Although lipid bilayers are apparent in most tubules, they are especially prominent in the bracketed region in E and in cross sections in inset marked by arrowheads. Arrows in E point to the apparent connection between the TMC and ER tubules. (F and G) TMCs contain the ER transmembrane protein Sec61β. BHK-21 cells stably expressing YFP-Sec61β were transfected to induce the formation of TMCs and stained with anti-DLP1 antibodies. TMCs shown in F are positive for YFP-Sec61β (G), indicating TMCs are comprised, in part, of ER membrane. N, nucleus; G, Golgi apparatus. Bars, 1.0 μm (A–C), 100 nm (D and E).

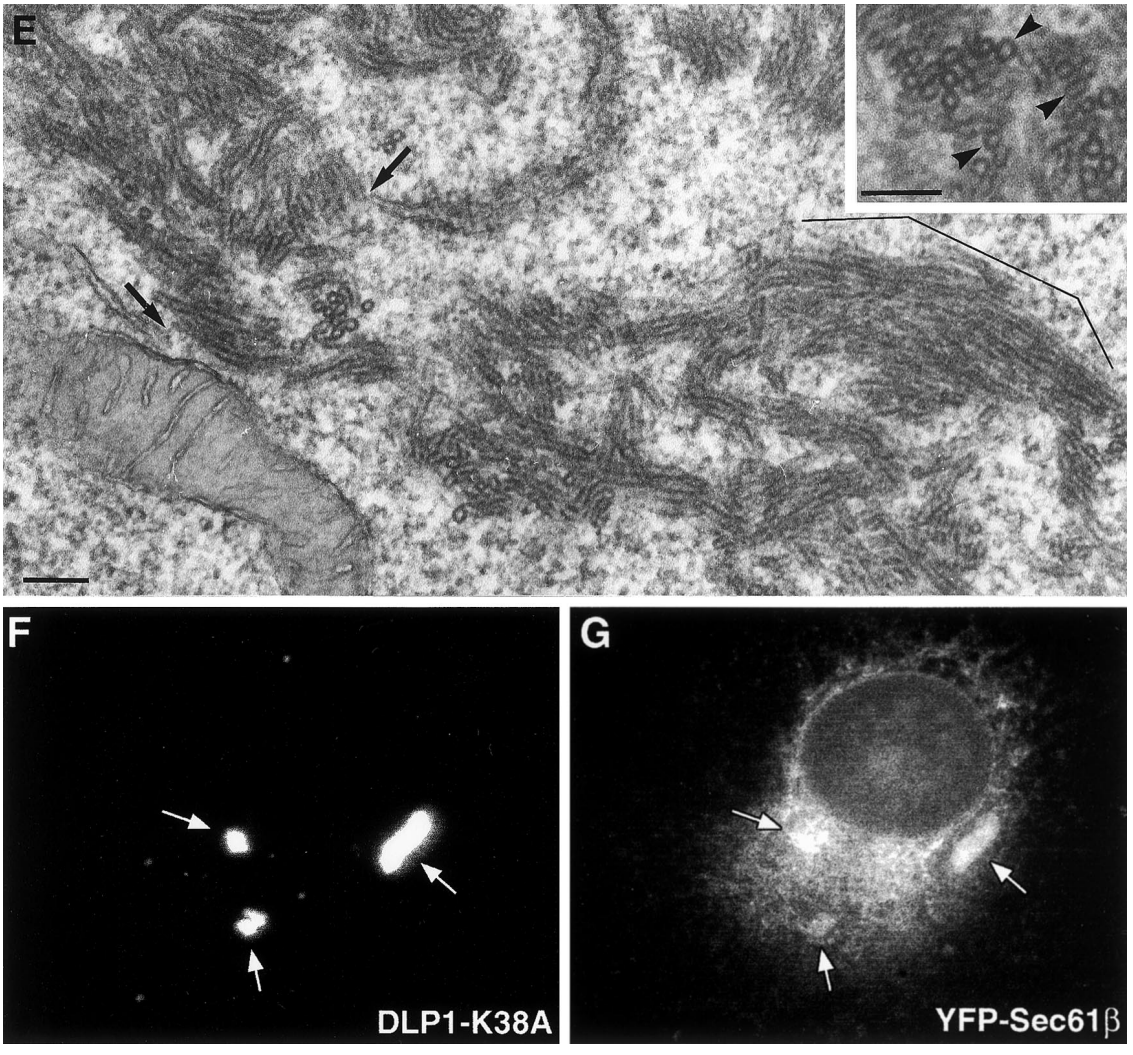

Figure 2 (legend on facing page).

DLP1-K38A in the pellet increased dramatically, whereas WT showed a modest increase in membrane-associated protein. Virtually all of the DLP1-K38A sedimented with membranes, whereas WT protein was distributed equally between the supernatant and pellet. These results support the prediction that the DLP1-K38A mutant protein associates with membranes more tightly presumably due to its prolonged GTP-bound state. Accordingly, like other GTPases, DLP1 exhibits a significant increase in its affinity for membranes when GTP bound.

DLP1 Deforms Spherical Liposomes into Elongated Tubules In Vitro

The formation of TMCs in DLP1-K38A mutant cells suggested that DLP1 might also induce lipid tubule formation in vitro, as demonstrated previously for conventional dynamin (Sweitzer and Hinshaw, 1998; Takei *et al.*, 1998, 1999). To reconstitute membrane tubulation by DLP1 in vitro, we used purified recombinant DLP1 in the presence or absence of synthetic liposomes. In the absence of lipid membranes, DLP1 protein assembled into sedimentable macromolecular structures (Figure 6A). This polymer formation was sensitive to GTP, because addition of GTP to the reaction mixture drastically reduced the amount of sedimentable DLP1. Furthermore, addition of GTPγS increased the amount of polymeric, sedimentable DLP1, suggesting that DLP1 assembly and disassembly are nucleotide-dependent. EM of GTPγS-treated DLP1 polymers revealed clusters of rings as well as cylindrical structures, presumably stacks of rings, whereas no ordered structures were found either in the absence of nucleotide or upon GTP addition. These polymers usually aggregated into clusters, exhibiting a honeycomb-like configuration when viewed en face (Figure 6B) or cylindrical stacks of rings by side view (Figure 6C). The formation of these clusters suggests that strong lateral interactions are present between concentric DLP1 stacks.

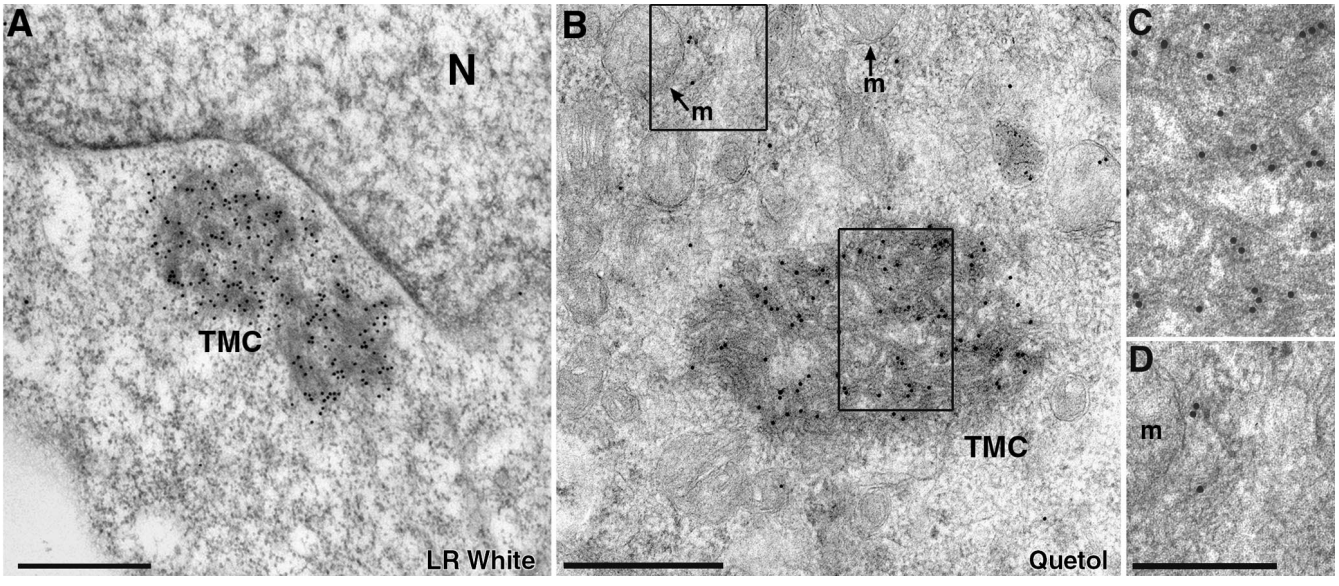

Figure 3. Tubular membrane clusters are comprised of DLP1. BHK-21 cells expressing GFP-DLP1-K38A were subjected to immunoelectron microscopy with an antibody against DLP1. Cells embedded in LR White display large perinuclear TMCs that label strongly with DLP1 antibodies (A). To better preserve the ultrastructure of the membrane tubules, cells were embedded in Quetol and then deplasticized before sectioning. In this preparation numerous gold particles can be seen along the membrane tubules comprising the TMC (B). Higher magnification images of boxed regions in B (C and D). Note that peripheral gold particles label membrane structures near, but not on, the mitochondria (D). N, nucleus; m, mitochondrion; Bars, 500 nm (A and B), 250 nm (C and D); gold, 15 nm.

Next, we tested whether DLP1 could tubulate membrane in a cell-free assay. Samples containing only extruded lipids without added DLP1 showed spherical liposomes of various sizes (Figure 7A). When DLP1 was included with liposomes prepared from either brain lipids or PS, long membrane tubules were occasionally observed by negative stain EM. Addition of GTPγS to the preparation greatly enhanced tubule formation (Figure 7, B–G), suggesting that the GTP-bound form of DLP1 more efficiently induces liposome tubulation, consistent with the in vivo findings for DLP1-K38A shown in Figure 2. The in vitro tubules possessed a consistent diameter of 31 ± 6 nm, comparable with those formed in vivo by DLP1-K38A (Figure 2). At higher magnification, closely aligned striations along the tubules were visible (Figure 7, D and F). These striations were more apparent on the GTPγS-induced tubules. Striations were also frequently found on the surface of large tubulating liposomes in the GTPγS-treated sample (Figure 7, E and G). Apparent enhancement of striations on both tubules and liposomes by GTPγS suggests that tight association and assembly of DLP1 on the liposome surface increase tubulation efficiency.

DISCUSSION

In this study we have provided morphological and biochemical evidence that the dynamin-like protein DLP1 has the capacity to polymerize into macromolecular structures while binding and tubulating membrane similar to conventional dynamin. The initial findings were obtained from the observation that cultured cells expressing a mutant DLP1 protein (DLP-K38A) were found to contain extensive cytoplasmic clusters of membrane tubules (Figures 1 and 2). These tubules were of a remarkably consistent diameter (27 ± 3 nm) and coated with dense ring-like striations that labeled strongly with DLP1 antibodies at both the light and ultrastructural levels (Figures 1 and 3). Consistent with these morphological observations, we found that the DLP1-K38A mutant protein was able to bind but not hydrolyze GTP (Figure 4) which resulted in an increased affinity for membranes (Figure 5). To extend these findings made in living cells, we utilized an in vitro assay comprised of defined components including recombinant DLP1, guanine nucleotides, and phospholipids. We observed that DLP1 is capable of forming oligomeric protein ring structures in the presence of GTPγS (Figure 6) that deform liposomes into tubules of a near identical diameter to that observed in living cells (Figures 2 and 7). These findings show for the first time that, despite the limited sequence homology with the conventional dynamin proteins (35%), DLP1 possesses the capacity to self-assemble while tubulating biological membranes.

Formation of Tubular Membrane Clusters in Cells Expressing a Mutant DLP1

In a previous study (Pitts *et al.*, 1999) we observed the formation of large cytoplasmic clusters in cultured cells expressing GFP-DLP1-K38A. Because these structures were highly fluorescent (Figure 1) we assumed they were comprised, at least in part, of the GFP-DLP1-K38A protein. With the use of conventional TEM (Figure 2) combined with immunogold labeling (Figure 3), we confirmed that these clusters were indeed comprised of membrane tubules tightly wrapped by DLP1 rings. These striated tubules are reminiscent of the dynamin-generated membrane tubules observed

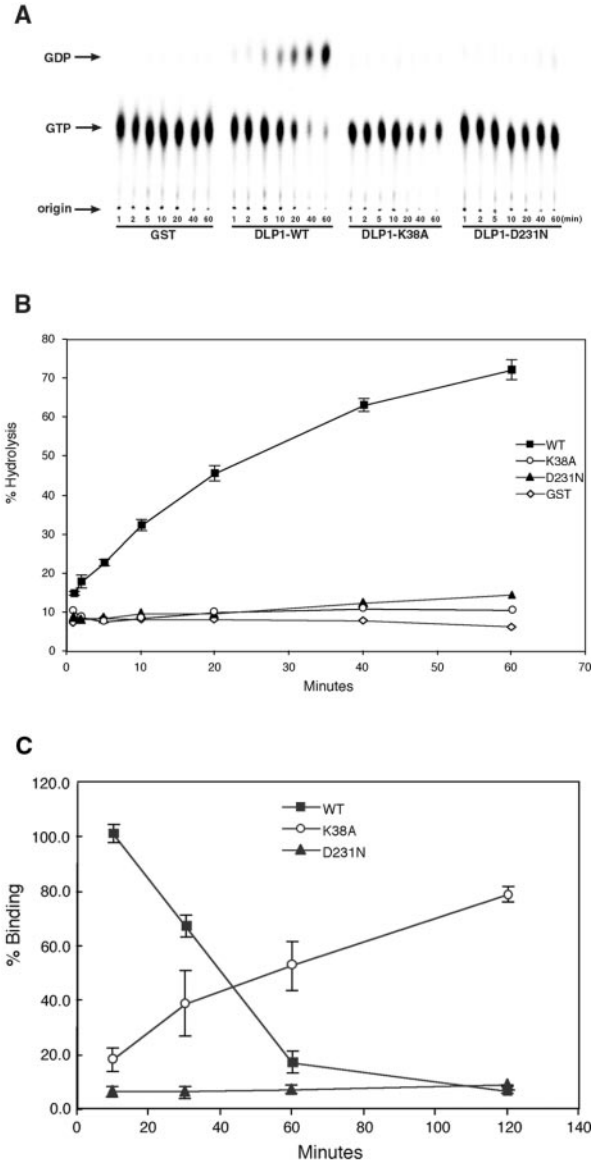

Figure 4. DLP1-K38A does not hydrolyze GTP and exhibits gradual accumulation of GTP. GTP hydrolysis assays were performed with WT and mutant DLP1 proteins. Purified GST-tagged WT and mutant proteins were incubated with [α-^{32}P]GTP for different time periods and then spotted onto a PEI-cellulose plate and separated by TLC (A). The ratio of GDP to total nucleotide (GDP + GTP) was plotted as a function of incubation time (B). Both the K38A and D231N mutations completely abolish DLP1 GTPase activity compared with WT-DLP1. (C) GTP binding of DLP1 WT and mutant proteins was tested with the use of GTP as a substrate. GST-tagged WT and mutant DLP1 were incubated with radiolabeled nucleotides for different periods of time. At each time point, GST-tagged proteins were recovered and washed to remove unbound nucleotide and bound nucleotide was measured by scintillation counting. Nucleotide binding was expressed as a percentage of nucleotide bound by WT protein at 10 min. Initially, WT shows higher GTP binding compared with DLP1-K38A and DLP1-D231N. As incubation time increases, WT-bound nucleotide decreases dramatically indicating that WT hydrolyzes and releases GTP over time, whereas DLP1-K38A accumulates nucleotide, suggesting that it is unable to release GTP. DLP1-K38A shows an 8–10-fold increase in GTP binding over WT after a 120-min incubation.

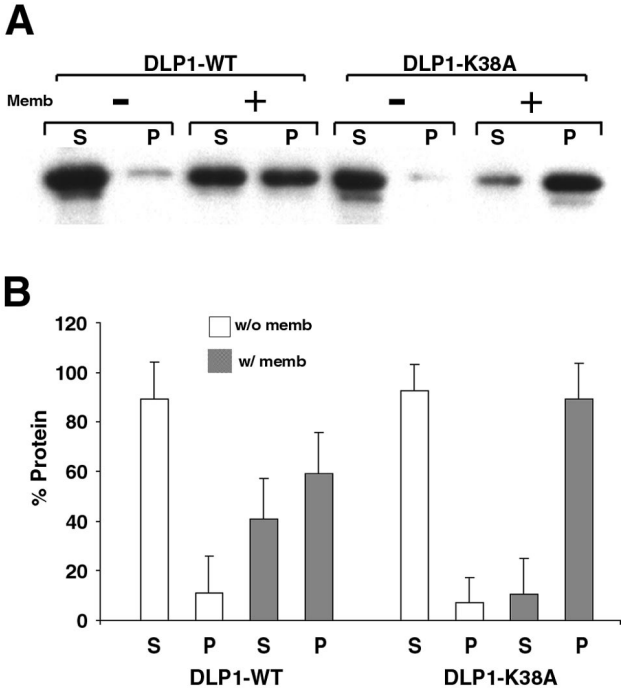

Figure 5. DLP1-K38A has a high affinity for membranes. (A) Purified GST-tagged proteins were incubated with or without carbonate-stripped total rat liver membranes in the presence of GTP. Reaction mixtures were centrifuged at 39,000 × *g* to separate supernatant and pellet, which were then subjected to immunoblot analyses with an anti-DLP1 antibody. In the absence of membranes, WT and DLP1-K38A proteins remain soluble in the supernatant. In the presence of membranes, similar amounts of protein are found in supernatant and pellet with WT protein. However, DLP1-K38A protein shows a high affinity for membranes with most of the protein found associated with the membrane pellet. (B) Densitometric analyses was performed with the use of three separate membrane-pelleting assays. In the absence of membranes, both WT and DLP1-K38A proteins are found in the supernatant (□). Addition of membranes to the reaction mixture results in a substantial increase of DLP1-K38A protein in the pellet compared with WT (■). S, supernatant; P, pellet.

in lysed synaptosomal preparations incubated with GTPγS (Takei *et al.*, 1995; Takei *et al.*, 1998; Takei *et al.*, 1999).

Recent studies of DLP1/DNM1 in mammalian cells (Smirnova *et al.*, 1998; Pitts *et al.*, 1999), yeast (Otsuga *et al.*, 1998; Bleazard *et al.*, 1999; Sesaki and Jensen, 1999), and nematode (Labrousse *et al.*, 1999) have provided evidence that DLP1 participates in mitochondrial morphogenesis and fission. Although the mechanism of this action is unclear at present, it has been postulated that DLP1 may act as a "mitochondrial pinchase" (Bleazard *et al.*, 1999; Labrousse *et al.*, 1999; Sesaki and Jensen, 1999). This model is supported by the fact that cells expressing mutant DLP1/DNM1 display long, continuous, mitochondria that appear to collapse toward the cell center. Furthermore, this protein has been morphologically localized to the sites of mitochondrial fission (Bleazard *et al.*, 1999). In contrast, others have suggested that DLP1 mutant cells are deficient in secretion of nascent proteins (Imoto *et al.*, 1998) or exhibit a marked loss of ER cisternae in addition to a mitochondrial phenotype (Pitts *et al.*, 1999).

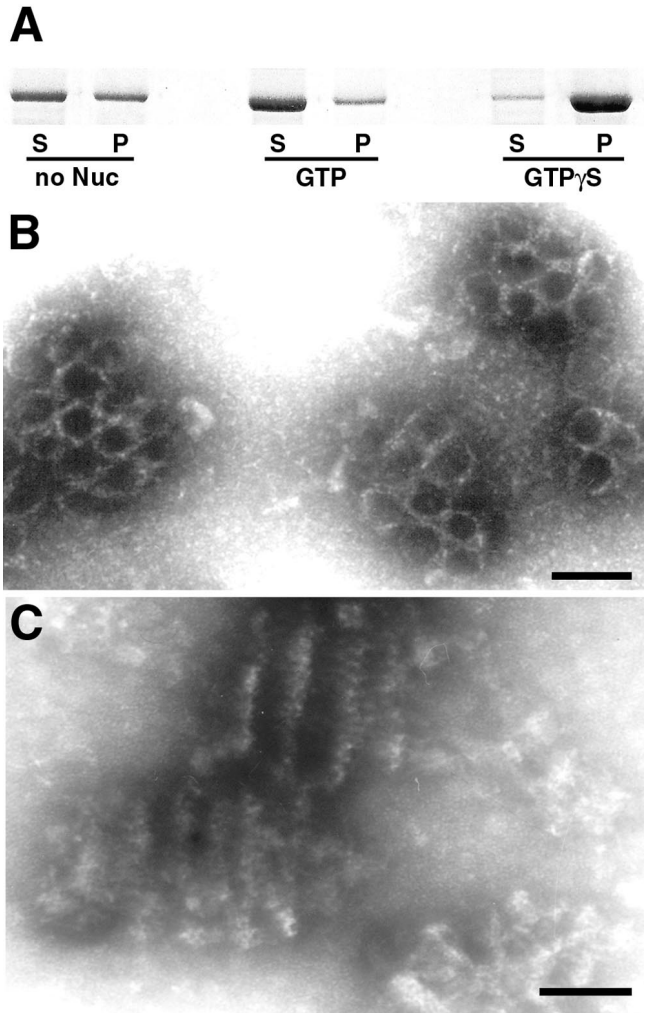

Figure 6. DLP1 assembles into macromolecular structures in a nucleotide-dependent manner. DLP1 assembles into sedimentable macromolecular structures (A). 6-His-tagged DLP1 was incubated with or without nucleotide and the reaction mixture was centrifuged at 100,000 × *g* to pellet assembled polymers. DLP1 polymer formation is apparently sensitive to GTP, because addition of GTP to the reaction mixture significantly reduces the amount of sedimentable DLP1 polymers (A). Furthermore, addition of GTPγS increases the amount of DLP1 in the polymeric form (A). Electron micrographs of GTPγS-treated DLP1 reveal clusters of rings as well as cylindrical structures, presumably stacks of rings (B and C), whereas no ordered structures are found either in the absence of nucleotide or in GTP-treated DLP1. Bars, 50 nm.

This is consistent with biochemical and morphological observations that only a small percentage of total cytoplasmic DLP1 associates with mitochondria proper, with the majority distributed to other cellular locations, including the microtubule cytoskeleton and ER cisternae (Yoon *et al.*, 1998; Pitts *et al.*, 1999). In an effort to define the source of the membranes within the DLP1 clusters we observed that TMCs are found to contain YFP-Sec61β, a main component of the protein translocation complex in the ER membrane, whereas no mitochondrial or Golgi membrane proteins are present in TMCs (Figure 2, F and G). These findings are consistent with the morphological ER defects observed in DLP1 mutant cells (Pitts *et al.*, 1999) and suggest that ER or mitochondrial morphology is maintained by DLP1-mediated events common to these two organelles. The electron microscopic observations of DLP1-K38A expressing cells summarized in Figure 2 show no mitochondrial profiles or remnants within the aggregates of membrane tubules. Instead, unusually long, isolated strands of rough ER can be seen in close association with the aggregates as if continuous with the tubules. Large areas of empty cytoplasm devoid of ER surround these structures. Finally, immunogold labeling of mutant cells with DLP1 antibodies (Figure 3) again reveals little antigen directly on mitochondria. Instead, gold particles are localized to the large tubular aggregates and to membranous structures in proximity to the mitochondria (Figure 3D). Although future studies will examine the biogenesis and content of these membrane structures, these current observations are consistent with the premise that DLP1, like conventional dynamin, possesses a high propensity to constrict and tubulate cytoplasmic membranes.

GTP-bound DLP1 Tubulates Membranes

To better understand the mechanisms supporting the DLP1–membrane interactions, we characterized the enzymatic properties of DLP1-K38A by testing how GTP binding and hydrolysis alter membrane association. As demonstrated in Figure 4, this mutant was unable to hydrolyze GTP as well as having reduced GTP binding. Further analyses revealed that this mutant does not release nucleotide due to its inability to hydrolyze bound GTP, thus locking it in a GTP-bound state. Within other proteins of the GTPase superfamily, up to five short peptide sequences (G-1 to G-5) have been identified as GTP-binding elements (Bourne *et al.*, 1991). Dynamins and DLP1 are known to have three of these consensus sequences, G-1, G-3, and G-4, and a recent report suggests the presence of a G-2 element in the dynamin family of proteins (van der Bliek, 1999). Based on comparison with the family of small GTPases (Bourne *et al.*, 1991), the K38A mutation in DLP1 is in the G-1 element that mediates interactions with nucleotide phosphate groups, whereas the D231N mutation is in G-4, a region known to confer nucleotide base specificity, associating with the guanine ring to stabilize binding. Thus, our observations are consistent with the premise that DLP1-K38A, a G-1 mutant, binds but does not hydrolyze GTP, whereas the G-4 DLP1-D231N mutant is completely deficient in GTP binding. Our GTP-binding experiments demonstrated that DLP1-K38A binds nucleotide to a lesser extent. However, it is also possible that the apparent slow binding of labeled GTP to DLP1-K38A shown in Figure 4C is due to slow dissociation of GTP already present in the protein because it is not known whether the DLP1 used in this binding study was already associated with nucleotides upon isolation. In either case, DLP1-K38A is capable of binding nucleotide and has a prolonged GTP-bound state. Based on the previous characterizations of other GTP-bound proteins that mediate membrane trafficking, we predict that DLP1 undergoes cycles of GTP binding, hydrolysis, and release that result in association and dissociation with cellular membranes. It has been established for Rab and ARF proteins that the GTP-bound form of the enzyme binds to membranes and, upon GTP

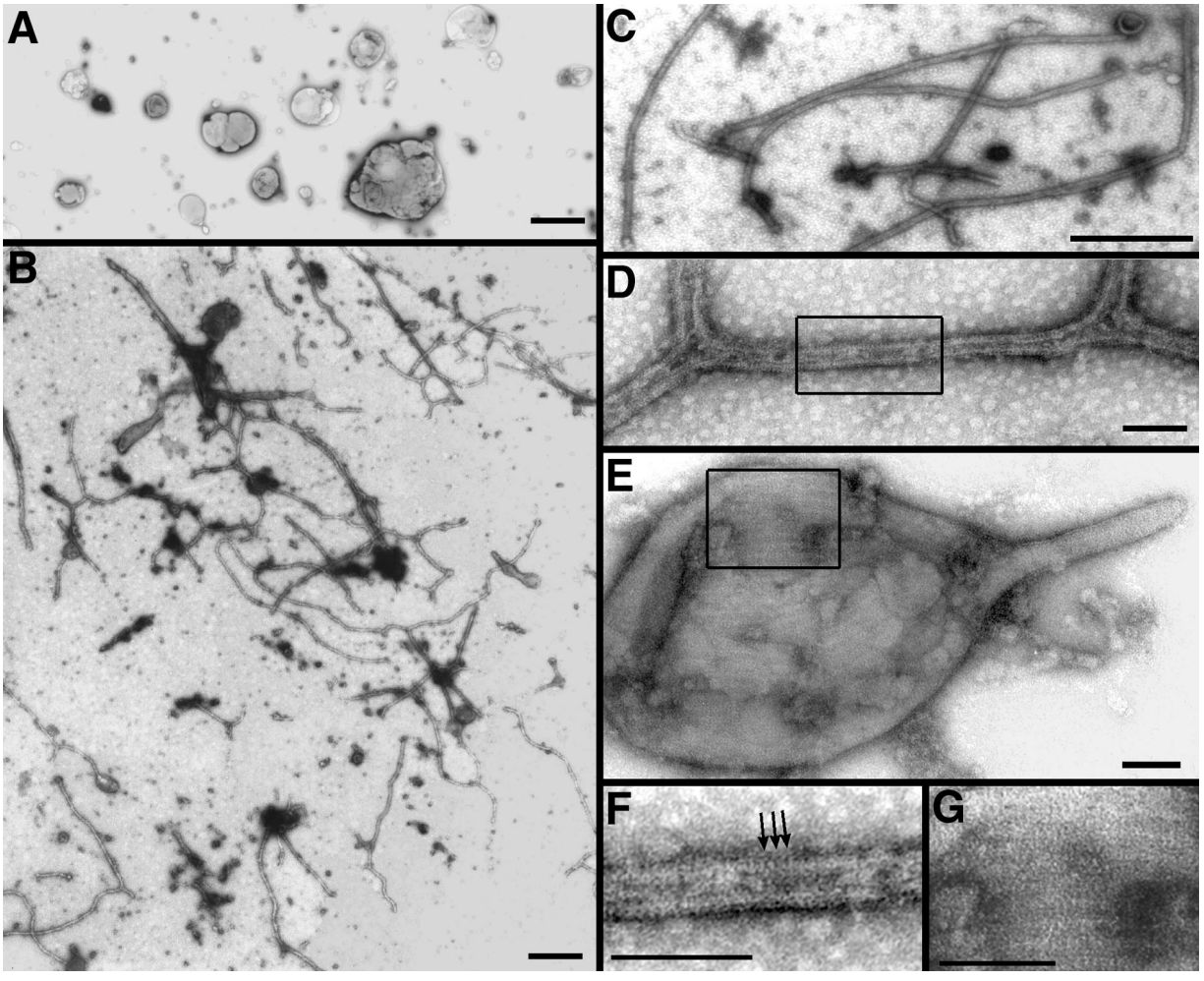

Figure 7. DLP1 deforms spherical liposomes into elongated tubules in vitro. Electron micrographs of negatively stained liposome preparations in the absence or presence of DLP1. PS liposomes in the absence of DLP1 are spherical and vary in size (A). PS liposomes incubated in the presence of recombinant 6-His-tagged DLP1 and GTPγS exhibited numerous long branched membrane tubules (B–D). Higher magnification (D and F) reveals closely aligned proteinaceous striations along the tubules (F, arrows). These striations are also present on tubulating liposomes (E) and are more pronounced at higher magnification (G). Bars, 1.0 μm (A), 500 nm (B and C), 50 nm (D–G).

hydrolysis and release, dissociates from membranes (Donaldson and Klausner, 1994; Pfeffer, 1994). As demonstrated in Figure 5, the GTPase cycle of DLP1 also appears to control membrane association. Our results indicate that DLP1-K38A is a GTPase-defective mutant locked in the GTP-bound state that, in turn, results in tight and prolonged association with membranes both in vitro (Figure 5) and in living cells (Figures 1 and 2). In contrast, the GTP-binding defective DLP1-D231N protein displays reduced membrane association in living cells showing a diffuse cytosolic distribution (Pitts *et al.*, 1999). Although these results suggest that DLP1 binds membranes in a nucleotide-sensitive manner, GTP binding may not be the direct cause of membrane association of this protein. It is possible that conformational changes induced by GTP binding may activate downstream events such as protein–protein interactions that subsequently lead to membrane association. Certainly, GTP hydrolysis by conventional dynamin induces conformational changes in the protein, resulting in a mechanical action (Sweitzer and Hinshaw, 1998; Takei *et al.*, 1998; Stowell *et al.*, 1999; Takei *et al.*, 1999; Marks *et al.*, 2001). However, it is not known whether GTP binding causes conformational changes in dynamin or DLP1 and further studies are necessary to elucidate this matter. In any case, according to our morphological data shown in Figure 7, it is likely that the GTP-bound form of DLP1 has increased membrane binding because GTPγS greatly enhances liposome-tubulating action by purified DLP1.

DLP1, Tubulating or Pinching Membrane?

The formation of tubulated membrane clusters encased by DLP1-K38A striations in living cells prompted us to test whether this protein could self-assemble into rings and tubulate membranes in vitro. By biochemical criteria (Figure 6) we found that DLP1 does indeed form sedimentable mac-

romolecular structures. This assembly is sensitive to GTP and accentuated by addition of GTPγS. Although sedimentable DLP1 protein can also be obtained in the absence of nucleotide, ordered structures of rings and ring stacks are found only with GTPγS-treated DLP1 as assessed by EM. These structures usually aggregate into large clusters (Figure 6), suggesting the presence of strong intermolecular lateral interactions.

In the presence of synthetic liposomes, we found that DLP1 is also able to deform spherical liposomes into long tubules like conventional dynamin. Although tubule morphology is similar to that formed by dynamin, branched tubules are frequently observed in preparations with DLP1. Striations on tubulating liposomes as well as on the branching regions of tubules are aligned in several different directions (Figure 7E), which may dictate the direction of tubulation or branching.

It has been reported that both dynamin self-assembly and liposome tubulation by dynamin are independent of nucleotide (Hinshaw and Schmid, 1995; Sweitzer and Hinshaw, 1998). However, we observed that GTP promotes disassembly of DLP1 polymers, whereas GTPγS induces formation of stacked rings. These data suggest that GTP binding to DLP1 causes concentric assembly of DLP1 and upon hydrolysis of GTP, DLP1 dissociates to smaller subunit forms. These smaller forms are likely to be soluble tetrameric structures, as suggested previously (Shin *et al.*, 1999). Presently, it is not clear whether GTP hydrolysis by DLP1 would cause fragmentation of tubules, as shown with conventional dynamin (Sweitzer and Hinshaw, 1998; Takei *et al.*, 1999). Although not many tubules are observed in the presence of GTP, it is not certain whether the lack of tubules is due to the fragmentation of tubules or inefficient tubulation. One way to test the vesiculation of tubules is by measuring the light scattering, which decreases upon tubule fragmentation (Sweitzer and Hinshaw, 1998; Takei *et al.*, 1999). However, inefficient tubulation of liposomes by DLP1 in the absence of GTPγS must first be experimentally overcome to test GTP-dependent fragmentation. Thus, whether DLP1 acts to tubulate or sever membrane in the confines of a living cell is yet to be determined.

The results presented here provide the first evidence that the dynamin family member DLP1 is able to self-assemble and tubulate membranes both in living cells and in vitro. Studies directed at elucidating the biological membrane and/or protein targets where DLP1 self-assembles, and how this assembly is regulated, will expand our understanding of DLP1 function.

ACKNOWLEDGMENTS

This work was supported by grants from the National Institute of Diabetes and Digestive and Kidney Diseases to Y.Y. (DK-02648) and to M.A.M. (DK-44650).

REFERENCES

Bleazard, W., McCaffery, J.M., King, E.J., Bale, S., Mozdy, A., Tieu, Q., Nunnari, J., and Shaw, J.M. (1999). The dynamin-related GTPase Dnm1 regulates mitochondrial fission in yeast. Nat. Cell Biol. *1*, 298–304.

Bourne, H.R., Sanders, D.A., and McCormick, F. (1991). The GTPase superfamily: conserved structure and molecular mechanism. Nature *349*, 117–127.

Damke, H., Baba, T., Warnock, D.E., and Schmid, S.L. (1994). Induction of mutant dynamin specifically blocks endocytic coated vesicle formation. J. Cell Biol. *127*, 915–934.

Donaldson, J.G., and Klausner, R.P. (1994). ARF: a key regulatory switch in membrane traffic and organelle structure. Curr. Opin. Cell Biol. *6*, 527–532.

Henley, J.R., Krueger, E.W.A., Oswald, B.J., and McNiven, M.A. (1998). Dynamin-mediated internalization of caveolae. J. Cell Biol. *141*, 85–99.

Henley, J.R., and McNiven, M.A. (1996). Association of a dynamin-like protein with the Golgi apparatus in mammalian cells. J. Cell Biol. *133*, 761–775.

Herskovits, J.S., Burgess, C.C., Obar, R.A., and Vallee, R.B. (1993). Effects of mutant rat dynamin on endocytosis. J. Cell Biol. *122*, 565–578.

Hinshaw, J.E., and Schmid, S.L. (1995). Dynamin self-assembles into rings suggesting a mechanism for coated vesicle budding. Nature *374*, 190–192.

Imoto, M., Tachibana, I., and Urrutia, R. (1998). Identification and functional characterization of a novel human protein highly related to the yeast dynamin-like GTPase Vps1p. J. Cell Sci. *111*, 1341–1349.

Jones, S.M., Howell, K.E., Henley, J.R., Cao, H., and McNiven, M.A. (1998). Role of dynamin in the formation of transport vesicles from the trans-Golgi network. Science *279*, 573–577.

Kamimoto, T., Nagai, Y., Onogi, H., Muro, Y., Wakabayashi, T., and Hagiwara, M. (1998). Dymple, a novel dynamin-like high molecular weight GTPase lacking a proline-rich carboxyl-terminal domain in mammalian cells. J. Biol. Chem. *273*, 1044–1051.

Labrousse, A.M., Zappaterra, M.D., Rube, D.A., and van der Bliek, A.M. (1999). *C. elegans* dynamin-related protein DRP-1 controls severing of the mitochondrial outer membrane. Mol Cell *4*, 815–826.

Llorente, A., Rapak, A., Schmid, S.L., Deurs, B.V., and Sandvig, K. (1998). Expression of mutant dynamin inhibits toxicity and transport of endocytosed ricin to the Golgi apparatus. J. Cell Biol. *140*, 553–563.

Maier, O., Knoblich, M., and Westermann, P. (1996). Dynamin II binds to the trans-Golgi network. Biochem. Biophys. Res. Commun. *223*, 229–233.

Marks, B., Stowell, M.H., Vallis, Y., Mills, I.G., Gibson, A., Hopkins, C.R., and McMahon, H.T. (2001). GTPase activity of dynamin and resulting conformation change are essential for endocytosis. Nature *410*, 231–235.

McNiven, M.A. (1998). Dynamin: a molecular motor with pinchase action. Cell *94*, 151–154.

McNiven, M.A., Cao, H., Pitts, K.R., and Yoon, Y. (2000). The dynamin family of mechanoenzymes. pinching in new places. Trends Biochem. Sci. *25*, 115–120.

Nicoziani, P., Vilhardt, F., Llorente, A., Hilout, L., Courtoy, P.J., Sandvig, K., and Deurs, B.V. (2000) Role for dynamin in late endosome dynamics, and trafficking of the cation-independent mannose 6-phosphate receptor. Mol. Biol. Cell *11*, 481–495.

Otsuga, D., Keegan, B.R., Brisch, E., Thatcher, J.W., Hermann, G.J., Bleazard, W., and Shaw, J.M. (1998). The dynamin-related GTPase, Dnm1p, controls mitochondrial morphology in yeast. J. Cell Biol. *143*, 333–349.

Pfeffer, S.R. (1994). Rab GTPases: master regulators of membrane trafficking. Curr. Opin. Cell Biol. *6*, 522–526.

Pitts, K.R., Yoon, Y., Krueger, E.W., and McNiven, M.A. (1999). The dynamin-like protein DLP1 is essential for normal distribution and morphology of the endoplasmic reticulum and mitochondria in mammalian cells. Mol. Biol. Cell *10*, 4403–4417.

Sesaki, H., and Jensen, R.E. (1999). Division versus fusion: Dnm1p and Fzo1p antagonistically regulate mitochondrial shape. J. Cell Biol. *147*, 699–706.

Sever, S., Muhlberg, A.B., and Schmid, S.L. (1999). Impairment of dynamin's GAP domain stimulates receptor-mediated endocytosis. Nature *398*, 481–486.

Shin, H.W., Shinotsuka, C., Torii, S., Murakami, K., and Nakayama, K. (1997). Identification and subcellular localization of a novel mammalian dynamin-related protein homologous to yeast Vps1p and Dnm1p. J. Biochem. *122*, 525–530.

Shin, H.W., Takatsu, H., Mukai, H., Munekata, E., Murakami, K., and Nakayama, K. (1999). Intermolecular and interdomain interactions of a dynamin-related GTP-binding protein, Dnm1p/Vps1p-like protein. J. Biol. Chem. *274*, 2780–2785.

Smirnova, E., Shurland, D.L., Ryazantsev, S.N., and van der Bliek, A.M. (1998). A human dynamin-related protein controls the distribution of mitochondria. J. Cell Biol. *143*, 351–358.

Stirling, J.W., and Graff, P.S. (1995). Antigen unmasking for immunoelectron microscopy: labeling is improved by treating with sodium ethoxide or sodium metaperiodate, then heating on retrieval medium. J. Histochem. Cytochem. *43*, 115–123.

Stowell, M.H.B., Marks, B., Wigge, P., and McMahon, H.T. (1999). Nucleotide-dependent conformational changes in dynamin: evidence for a mechanochemical molecular spring. Nat. Cell Biol. *1*, 27–32.

Sweitzer, S.M., and Hinshaw, J.E. (1998). Dynamin undergoes a GTP-dependent conformational change causing vesiculation. Cell *93*, 1021–1029.

Takei, K., Haucke, V., Slepnev, V., Farsad, K., Salazar, M., Chen, H., and Camilli, P.D. (1998). Generation of coated intermediates of clathrin-mediated endocytosis on protein-free liposomes. Cell *94*, 131–141.

Takei, K., McPherson, P.S., Schmid, S.L., and De Camilli, P. (1995). Tubular membrane invaginations coated by dynamin rings are induced by GTP-γS in nerve terminals. Nature *374*, 186–190.

Takei, K., Slepnev, V., Haucke, V., and Camilli, P.D. (1999). Functional partnership between amphiphysin and dynamin in clathrin-mediated endocytosis. Nat. Cell Biol. *1*, 33–39.

van der Bliek, A.M. (1999). Functional diversity in the dynamin family. Trends Cell Biol. *9*, 96–102.

van der Bliek, A.M., Redelmeier, T.E., Damke, H., Tisdale, E.J., Meyerowitz, E.M., and Schmid, S.L. (1993). Mutations in human dynamin block an intermediate stage in coated vesicle formation. J. Cell Biol. *122*, 553–563.

Yoon, Y., Pitts, K.R., Dahan, S., and McNiven, M.A. (1998). A novel dynamin-like protein associates with cytoplasmic vesicles and tubules of the endoplasmic reticulum in mammalian cells. J. Cell Biol. *140*, 779–793.